

## NCAR'S NEW RAMAN-SHIFTED EYE-SAFE AEROSOL LIDAR (REAL)

Shane D. Mayor, Scott M. Spuler, Bruce M. Morley

National Center for Atmospheric Research  
Atmospheric Technology Division  
P.O. Box 3000, Boulder, Colorado, 80307-3000, USA

### ABSTRACT

The design features of, and first observations from, a new eye-safe elastic backscatter lidar system operating at a wavelength of  $1.54 \mu\text{m}$  are presented. Unlike previous lidar transmitters using stimulated Raman scattering in methane, the pump beam is not focused and the cell is injection seeded to improve conversion efficiency and beam quality. The receiver uses custom focusing optics and a  $200\text{-}\mu\text{m}$  diameter InGaAs avalanche photodiode (APD). An important achievement was reducing the transmit beam divergence so that it was smaller than the field-of-view (FOV) subtended by the receiver.

The first results were obtained by operating the system in a non-eye-safe dual-wavelength mode ( $1.064 \mu\text{m}$  and  $1.543 \mu\text{m}$  simultaneously). Single-wavelength eye-safe operation is achieved by the use of a prism to separate and block the  $1.064 \mu\text{m}$  beam before transmitting into the atmosphere. We are currently developing depolarization ratio measurement capability for use when pointing vertical and a beam steering unit for applications requiring scanning. The system is capable of transmitting over 200 mJ/pulse at 10 Hz at  $1.543 \mu\text{m}$ . Examples of backscatter data from vertical and horizontal pointing periods are shown.

### 1. MOTIVATION

Since January of 2002, NCAR's Atmospheric Technology Division has been developing an eye-safe aerosol backscatter lidar at  $1.54 \mu\text{m}$  wavelength. The original goal of the project was to produce a completely eye-safe aerosol backscatter lidar that could be deployed in atmospheric research field campaigns to monitor vertical profiles of aerosol backscatter in the lower troposphere. We have far surpassed our original goal by producing sufficient power to see aerosol structures at 10 km range when pointed almost horizontally. This success has inspired us to move towards scanning and depolarization ratio measurement capabilities. We expect to complete our first field demonstrations in a mobile seater during the spring and summer of 2004. A more complete description of the transmitter and receiver can be found in Mayor et al.[1]

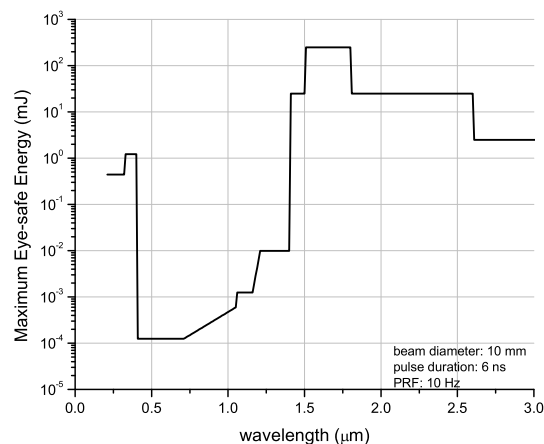


Figure 1. Maximum eye-safe energy as a function of wavelength for a 10 mm diameter beam, 6 ns pulse duration, and 10 Hz pulse repetition frequency.

Figure 1 shows the maximum eye-safe energy[2] (maximum permissible exposure times the beam area) for a pulsed laser as a function of beam wavelength. The chart shows that the region between  $1.5$  and  $1.8 \mu\text{m}$  has the highest permissible energy. With modest beam expansion it is possible to safely transmit over 1 J per pulse in this region. REAL's transmit beam diameter is approximately 10 cm at the exit aperture.

### 2. TRANSMITTER

The lidar transmitter begins with a flash-lamp pumped, Q-switched, Nd:YAG laser capable of generating 800 mJ/pulse energy at  $1.064 \mu\text{m}$  wavelength. The pump beam is converted to the eye-safe wavelength via stimulated Raman scattering (SRS) in a high pressure cell filled with pure  $\text{CH}_4$ . SRS is a third-order, nonlinear, inelastic scattering process whereby a sufficiently-high pump field excites molecular vibrations in a medium. The frequency of the scattered light (Stokes output) is shifted by the frequency of these vibrations. The Stokes field is initiated by the spontaneous emission of a photon and therefore the energy and spatial characteristics will fluctuate. To

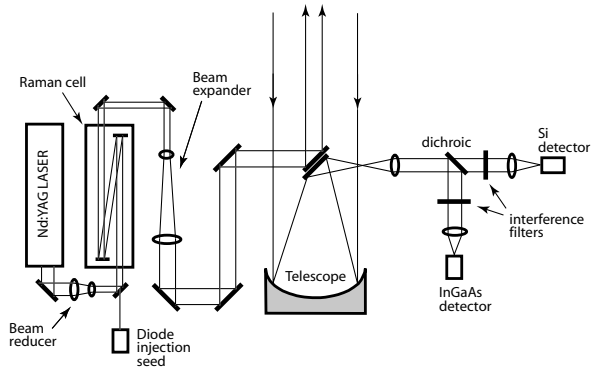


Figure 2. System schematic with Newtonian telescope. The data presented in this paper were collected with a Schmidt-Cassegrain telescope, but that has since been replaced with a 40 cm diameter custom Newtonian.

avoid these fluctuations one can seed the cell with a stable tunable Stokes wavelength laser. We injection seed our Raman cell with a continuous-wave 20 mW telecom diode laser which is coupled to a single mode fiber which emits a near perfect Gaussian beam.

The Raman cell was custom built and improved from the design of Kurnit et al.[3]. The internal mirrors have a high reflectivity coating at  $1.064 \mu\text{m}$  and  $1.540 \mu\text{m}$  and high transmission at the second Stokes line ( $2.8 \mu\text{m}$ ) and the first anti-Stokes line ( $0.81 \mu\text{m}$ ) to suppress build-up at these wavelengths. It is important to note, however, that the pump beam is *not* focused in the cell. Focusing a high energy beam in methane, often causes optical breakdown and leaves carbon/soot deposits on mirrors and windows—limiting long term operation of the transmitter.[4; 5] Internal fans circulate the methane. A diagram of the experimental setup is shown in Fig. 2.

### 3. RECEIVER

For the results presented here, our lidar receiver used a commercially available 40 cm diameter  $f/10$  Schmidt-Cassegrain telescope. The telescope is mounted in a fixed vertical position on an optics table. The backscatter light collected by the telescope is collimated with a doublet lens to facilitate transmission through subsequent interference filters. The lens is followed by a short-wave-pass dichroic to separate  $1.064 \mu\text{m}$  and  $1.543 \mu\text{m}$  backscatter. Both wavelengths are filtered by a narrow band pass interference filter to reject background light. The  $1.064 \mu\text{m}$  light passing through its filter is focused, via a single element aspheric lens, onto a 1.5 mm diameter active area, long wavelength enhanced, silicon APD. A custom focusing lens was designed to focus the eye-safe backscatter onto a photodiode. The lens is a three element design, a doublet with companion meniscus lens, with a 18 mm focal length and 12.4 mm diameter. The lens was designed

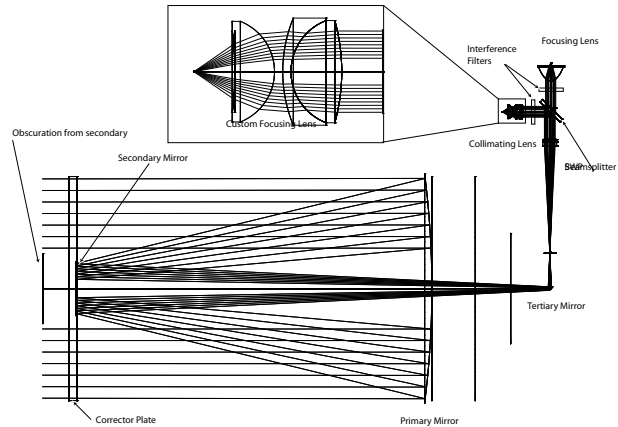


Figure 3. Ray-trace of the receiver for the dual-wavelength system configuration.

to collect all light within a  $0.50 \text{ mrad}$  full-angle onto the detector for the ranges 500 m to 15 km. In practice, the useful range of the instrument is slightly adjustable—analogueous to the depth-of-field of a camera. The photodetector is a  $200 \mu\text{m}$  diameter InGaAs/InP APD with 75% quantum efficiency and a bandwidth of 200 MHz.

Backscattered photons are converted to electrons by the photodetectors and the resulting electrical signals are amplified and digitized. For the  $1.064 \mu\text{m}$  channel, the detector package uses a 10 MHz bandwidth linear transimpedance amplifier. Prior to the this time of this writing, the  $1.543 \mu\text{m}$  signal is amplified by an operational amplifier that has a bandwidth of 55 MHz at a gain of 20. In order to amplify return signals that are near the noise level of the detector we operate the with a gain of approximately 850 which reduces the bandwidth to approximately 1 MHz. We are currently in the process of replacing that detector and amplifier with a Perkin Elmer C30659-1500-R2A InGaAs APD/preamplifier combination module with 50 MHz bandwidth.

Several factors can limit the range resolving capability of a backscatter lidar system. The  $1.543 \mu\text{m}$  pulse duration is 4 ns which corresponds to 1.2 m in space. The InGaAs APD has a bandwidth of 200 MHz with an equivalent rise time of 1.8 ns which corresponds to approximately 30 cm in range. However, as stated earlier, the bandwidth of our present amplifier is 1 MHz with an equivalent rise time of 350 ns which corresponds to approximately 53 m in range. The digitizer sampling rate controls the spacing of the data points despite they may not be independent samples due to one of the slower previous components. Our digitizer is capable of 100 MSPS in single-channel mode, however we typically use it in a 50 MSPS dual-channel mode. 50 MSPS is equivalent to 3 m spatial sampling. We expect the new Perkin Elmer C30659-1500-R2A to improve our range resolution to about 3 m.

## 4. DEPOLARIZATION

The ability to discern liquid water droplets from ice crystals is useful in studies of clouds and well documented[6]. We are in the process of adding this capability to REAL. In order to do it, we first had to improve the polarization purity of our pump laser by passing the light through a thin film plate resulting in a 200:1 polarization ratio which is improved from 70%. Unfortunately, we loose about 150 mJ/pulse of the pump. This in turn reduces the total transmit power at 1.54  $\mu\text{m}$  to approximately 170 mJ/pulse.

In the receiver we use a custom calcite polarization beam-splitter cube to separate the orthogonal polarization states. The cube is 25.5 mm clear aperture and results in 200,000:1 separation ratio. We will use two identical detector systems to measure the depolarization ratio at 50 MHz per channel.

## 5. BEAM STEERING UNIT

At the time of this writing, a beam steering unit (BSU) was being constructed for the lidar system. The BSU features a 17" clear aperture and capability to make full azimuth and elevation scans. The horizontal collar of the BSU contains a 16 channel slip-ring to transmit power to and exchange data with the elevation drive. This features allows continuous PPI type scans in one direction. Computer controlled motors (Animatic) with angle encoding allow full control and feedback of the mirror positions.

A ray-trace analysis of the receiver indicates that each BSU mirror must be flat to within 3 waves (0.9  $\mu\text{m}$  of sag) across the full aperture. This flatness tolerance is relaxed compared to most optical surfaces, but sufficient because lidar systems are non-imaging. The flatness requirement was driven mainly by the detector diameter, and to a lesser degree the other optics in the receiver sub-system. We have chosen Zerodur as the substrate material and protected gold-coatings for wavelength flexibility and high reflectivity in the 1.5  $\mu\text{m}$  region.

## 6. RESULTS AND DISCUSSION

The highest Stokes energy was obtained with a 3.4 m interaction length at a pressure of approximately 10 atm. In this configuration, 1.543  $\mu\text{m}$  energies in excess of 250 mJ/pulse were measured corresponding to better than 45% photon conversion efficiency. A significant enhancement of Stokes conversion efficiency, particularly at lower pressures, was seen with injection seeding and beam  $M^2$  was improved from  $\sim 16$  to  $\sim 11$ . The improvement in beam quality factor was critical for full overlap with our receiver system.

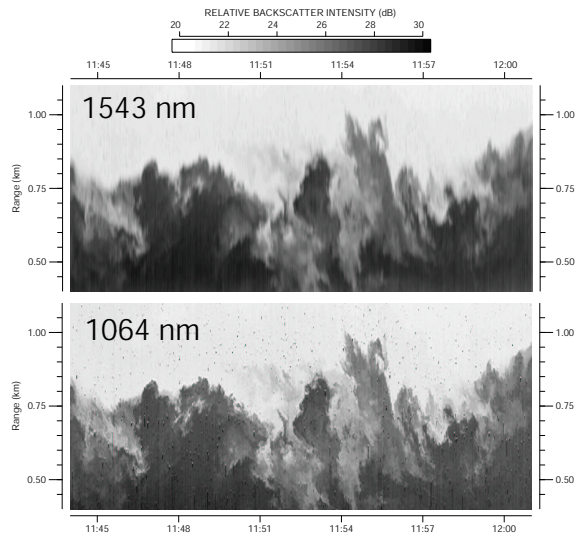


Figure 4. 17 minute by 700 m time-versus-altitude images of backscatter intensity from 1.54  $\mu\text{m}$  (top) and 1.064  $\mu\text{m}$  (bottom). The data of the entrainment zone were collected on 10 July 2003 in Boulder, CO.

When collecting data with the 1.064  $\mu\text{m}$  wavelength from our laboratory, we use a vertically pointed 3-cm wavelength Doppler radar for safety.[7] The radar provides a cone of microwave radiation surrounding the transmit beam. Software algorithms that identify aircraft echoes in the radar return turn off the laser immediately if an aircraft is detected.

In the data shown here, we have averaged together backscatter from consecutive groups of 10 laser shots to form 1 s averages. The backscatter signals were sampled at 50 MHz to provide data points at 3 m intervals in range. The DC baseline of each average return, which is proportional to the background intensity, is subtracted based on an average of data points sampled before the laser is fired. The average lidar return is then corrected for one-over-range-squared dependence. Figure 4 shows the backscatter intensity for the 1.543  $\mu\text{m}$  and 1.064  $\mu\text{m}$  wavelengths collected simultaneously when the beam was pointed vertically. Both images in Fig. 4 show the detailed vertical structure of the entrainment zone of a convective boundary layer. A visual comparison of the time-versus height images indicate the 1.54  $\mu\text{m}$  data are smoother. We attribute this to the bandwidth difference of the amplifiers of the two channels. Despite this difference, the comparison shows excellent agreement and demonstrates the ability to resolve fine scale detail at the eye-safe wavelength.

An important achievement was the ability to generate high energy pulses with good spatial quality. The receive FOV was severely restricted by the small diameter detector that we used. Therefore, steps were taken to minimize transmit beam divergence, maximize the receive FOV, and minimize the range of achieving full overlap. These included (1) coaxial transmit beam and receive FOV; (2)

injection seeding of Raman cell; (3) transmit beam expander; and (4) custom focusing optics in front of the detector.

## ACKNOWLEDGMENTS

We thank Tim Rucker and Eric Loew for assistance with lab work and electrical engineering, Dr. Dirk Richter for guidance regarding the diode laser and electronics, Jack Fox for design of the Raman cell, and Steve Rauenbuehler for design of the BSU. NCAR is sponsored by the U.S. National Science Foundation (NSF). This work was also supported by the U.S. Department of Energy, under the auspices of the Environmental Meteorology Program of the Office of Biological and Environmental Research (DEFG02-04ER63706). Additional funds from the Defense Advanced Research Projects Agency (DARPA) were provided for field testing the scanning capability.

## REFERENCES

1. Mayor, S. D., Spuler, S. M., and Morley, B. M. Raman-shifted eye-safe aerosol lidar (real). *Appl. Optics*, 2004 (In press).
2. ANSI. *American National Standard for the Safe Use of Lasers*, page 120. American National Standards Institute, 1993.
3. Kurnit, N. A., Harrison, R. F., Karl-Jr., R. R., Brucker, J. P., Busse, J., Grace, W. K., Peterson, O. G., Baird, W., and Hungate, W. S. Generation of 1.54 micron radiation with application to an eye-safe laser lidar. In *Proceedings of the International Conference on LASERS '97*, pages 608–610, 1997.
4. Carnuth, W. and Trickl, T. A powerful eyesafe infrared aerosol lidar: Application of stimulated raman backscattering of 1.06 micron radiation. *Rev. Sci. Instrum.*, 65:3324–3331, 1994.
5. Patterson, E. M., Roberts, D. W., and Gimmestad, G. G. Initial measurements using a 1.54 micron eye-safe raman shifted lidar. *Appl. Optics*, 28:4978–4981, 1989.
6. Sassen, K. The polarization lidar technique for cloud research: a review and current assessment. *Bull. Amer. Meteor. Soc.*, 72:1848–1866, 1991.
7. Gray, G. R. and Pratte, F. An eye-safety radar for lidar operations. In *AMS 31st International Conference on Radar Meteorology*, page P5B.9, Boston, 2003.

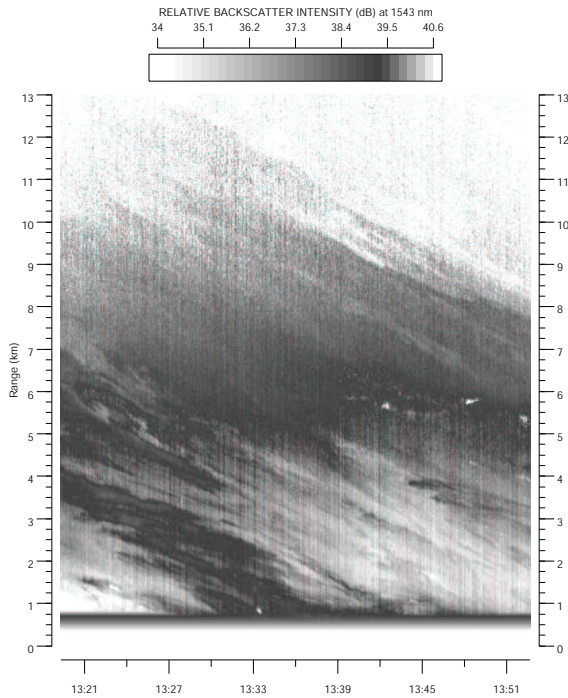


Figure 5. 30 minute by 13 km time-versus-range image of backscatter intensity at  $1.54 \mu\text{m}$ . The data were collected on 18 July 2003 in Boulder, Colorado, when the beam was pointed in a fixed near-horizontal position of  $3^\circ$  elevation angle.

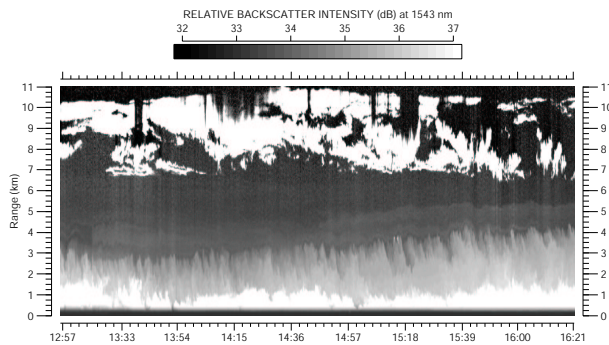


Figure 6. 5.5 hour by 11 km time-versus-altitude image of backscatter intensity at  $1.54 \mu\text{m}$  wavelength. The data were collected on 15 October 2003 in Boulder, Colorado. Turbulence is evident in the aerosol structure below approximately 4 km and complex cloud structure between 6.5 and 11 km.